

## Production and characterisation of electrolytically doped manganese dioxide

L. Binder <sup>a,\*</sup>, W. Jantscher <sup>a</sup>, F. Hofer <sup>b</sup>, G. Kothleitner <sup>b</sup>

<sup>a</sup> *Institut für Chemische Technologie Anorganischer Stoffe, Technical University Graz, Stremayrgasse 16, 8010 Graz, Austria*

<sup>b</sup> *Forschungsinstitut für Elektronenmikroskopie und Feinstrukturforchung, Technical University Graz, Steyrergasse 17, 8010 Graz, Austria*

Received 17 October 1996; revised 20 December 1996; accepted 27 January 1997

### Abstract

A laboratory batch process for the production of titanium-doped electrolytic manganese dioxide (EMD) in the amount of some hundred grammes is described. The product is characterised by chemical analysis, electrochemical behaviour, X-ray diffraction, and electron microscopy (TEM, ESI) including local electron energy loss spectroscopy (EELS) analysis. Suggestions for possible improvement of the doping process and for the preparation of the product are given. © 1998 Elsevier Science S.A.

*Keywords:* Manganese dioxide, electrolytic; Titanium doping

### 1. Introduction

Electrolytic manganese dioxide (EMD) is the most common variety of manganese dioxide used in primary Zn–MnO<sub>2</sub> batteries as the major component of composite cathodes. Despite the success of EMD as a primary battery material, the use of manganese dioxide as a secondary battery constituent has, for a few decades, met little success. The development of practically rechargeable alkaline manganese dioxide (RAM) cells has been performed by Kordesch [1–3] and by Battery Technologies, Ont., Canada. RAM-cells have been released onto the consumer market in 1993. The rechargeability of these batteries depends on a partial discharge of the manganese dioxide cathode. The discharge is limited to 35% of the theoretical one-electron capacity. This is achieved by limiting the anode capacity of the battery. Under these conditions one avoids the problems associated with manganese dioxide deep-discharge. The partially reduced species formed on discharge can be recharged to their original form in the charge cycle.

The batteries exhibit a correlation between the possible depth-of-discharge (DOD) and the number of charge/dis-

charge cycles (cycle life). Many attempts were made to improve DOD and cycle life. Evidently there is a correlation between structural parameters of the MnO<sub>2</sub> and its rechargeability. To improve the latter, physically or chemically modified manganese dioxide materials have been prepared. Most of the work has been concentrated on electrode materials doped with Bi or Pb ions by mixing EMD with suitable oxides [4], by co-pre-precipitation [5–7], or by impregnation/precipitation using aqueous solutions containing the required ions [8].

Another potential candidate for stabilising the structure of EMD is the Ti(IV) ion [9]. EMD is generally produced by anodic deposition using acidified aqueous solutions of manganese(II) sulfate. The direct introduction of titanium ions into the lattice of EMD by co-deposition can be managed. The cathodic deposition of the metal does not take place in aqueous media. Kordesch and Gsellmann [9] added soluble Ti(IV)-compounds, recovered from TiO<sub>2</sub> and TiS<sub>2</sub>, to the electrolytic bath. Ti(IV) halides can also be used as the additives to the electrolyte [10]. The content of titanium found in the manganese dioxide was up to 3%. Half-cell experiments showed an increase in number of possible cycles of over 100% compared with standard EMDs (International Common Samples). In this work an organotitanium compound, tetrabutyltitanate Ti(OBu)<sub>4</sub>, was used as an additive to the electrolyte according to previous experiments done by Urdl [10]. Tetrabutyltitanate is stable

\* Corresponding author: Tel.: +1 43-316-873-8263; Fax: +1 43-316-873-8272; e-mail: f537bind@mbox.tu-graz.ac.at

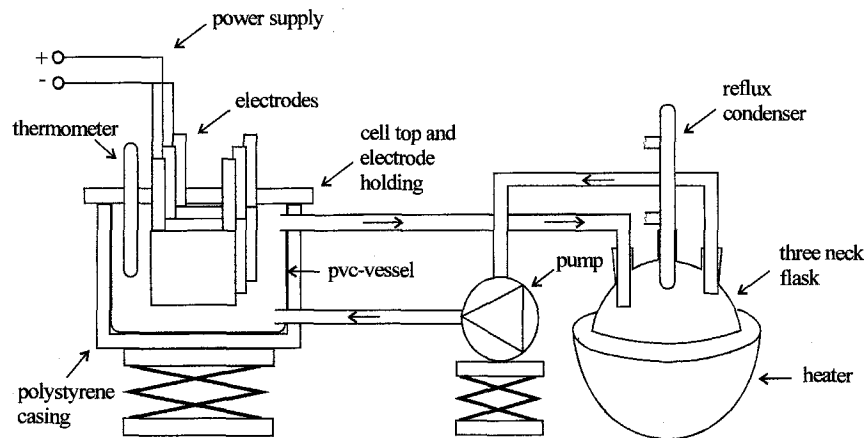


Fig. 1. Laboratory electrolyser for the production of titanium-doped EMD.

in air and soluble in acidified aqueous solution. It is of practical interest that this compound is easy to handle.

## 2. Experimental

### 2.1. EMD preparation

For the production of titanium-doped EMD on a laboratory scale a special electrolyser was built, see Fig. 1.

It consisted of a polyvinyl chloride (PVC) cell container (filled with up to 10 l electrolyte) and was equipped with a three-electrode system (one anode, two cathodes) fixed in a PVC support mounted on the cell top. The electrical connections as well as the electrodes were made from lead. To prevent heat loss, the cell was insulated using an outer shell made from foamed polystyrene. The electrolyte was externally heated in a three-neck flask equipped with a reflux condenser. The tubes leading from the cell to the magnetically coupled centrifugal pump and to the heating

device were made from PVC-C, a higher chlorinated PVC type with excellent corrosion resistance. Heating was done electrically and the bath temperature was remotely controlled. EMD was prepared by the standard procedure. The anode area was 10 dm<sup>2</sup> and the current was adjusted to 8 A (galvanostatic operation) giving a current density of 0.8 A dm<sup>-2</sup>. The cell voltage usually floated between 2.6 and 2.9 V. The process (one batch) was run for approximately 20 h. EMD deposits were mechanically removed from the anode, rinsed with water and dried. The EMD was ground with mortar and pestle. The resulting powder was suspended in distilled water and neutralised with ammonia solution. The supernatant was decanted and the EMD was repeatedly washed with distilled water. The product can be sieved, mixed with graphite and/or acetylene black and compacted (pressed) to cathode pellets.

### 2.2. Analyses

The titanium levels in EMD samples were measured by atomic absorption spectroscopy (AAS) and photometri-

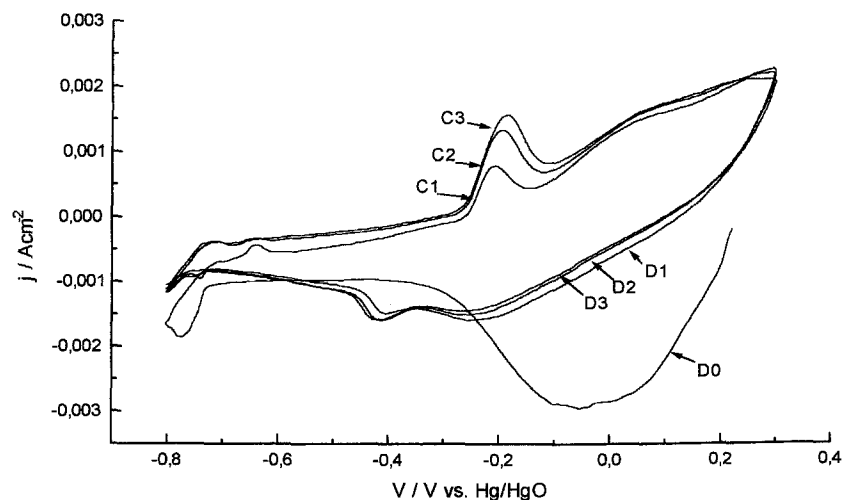


Fig. 2. Cyclic voltammogram of a titanium-doped EMD electrode: (D) discharge half cycle, and (C) charge half cycle.

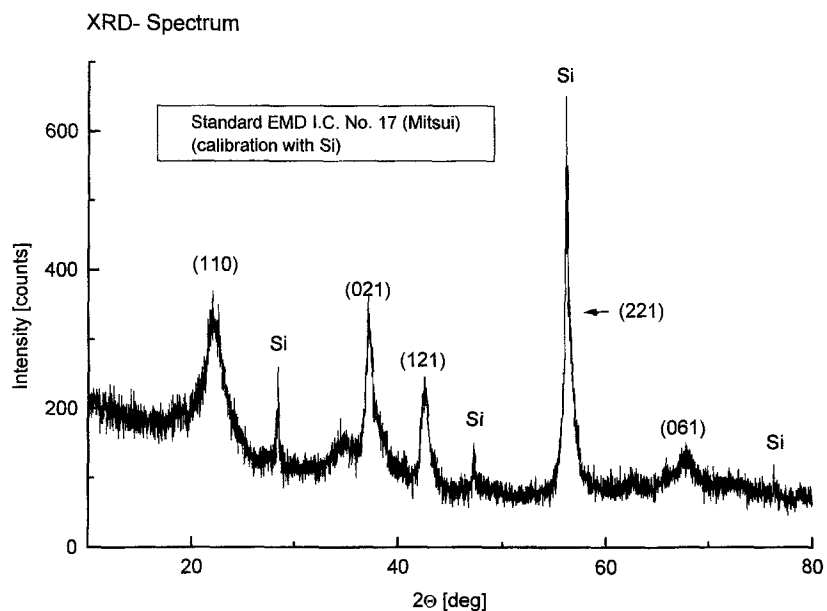


Fig. 3. X-ray diffraction pattern of standard EMD (I.C. sample no. 17).

cally. Cyclic voltammetry (CV) experiments were performed with a computer-controlled potentiostat-galvanostat Tacussel PJT 35-2, see Fig. 2. For CV experiments the EMD was ground and sieved through a 125 mesh screen. 0.5 ml of a 3% w/w polysulfone solution was added to 500 mg of a mixture of 80% w/w EMD with 20% w/w graphite (Lonza KS-44). Pellets were prepared by pressing samples of EMD mixtures on a nickel wire. Pellets were accurately weighed prior to each experiment. All potentials are referenced to a Hg/HgO (5 N KOH) electrode and a

platinum screen served as a counter electrode. Pellets were imbibed, in vacuum, with 9 N KOH for 4 h prior to each experiment. Experiments were run with a scan rate of 250–500  $\mu\text{V/s}$  in a potential range between  $-800$  and  $+300$  mV.

### 2.3. Electrochemical performance

Testing of the titanium-doped EMD will be done at Battery Technology, Canada. For this purpose AA cells

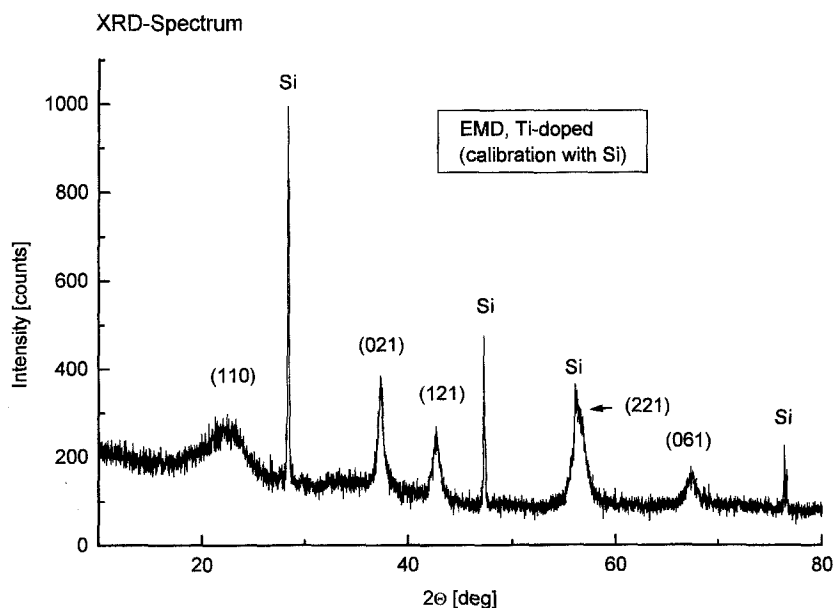


Fig. 4. X-ray diffraction pattern of titanium-doped EMD (laboratory product).

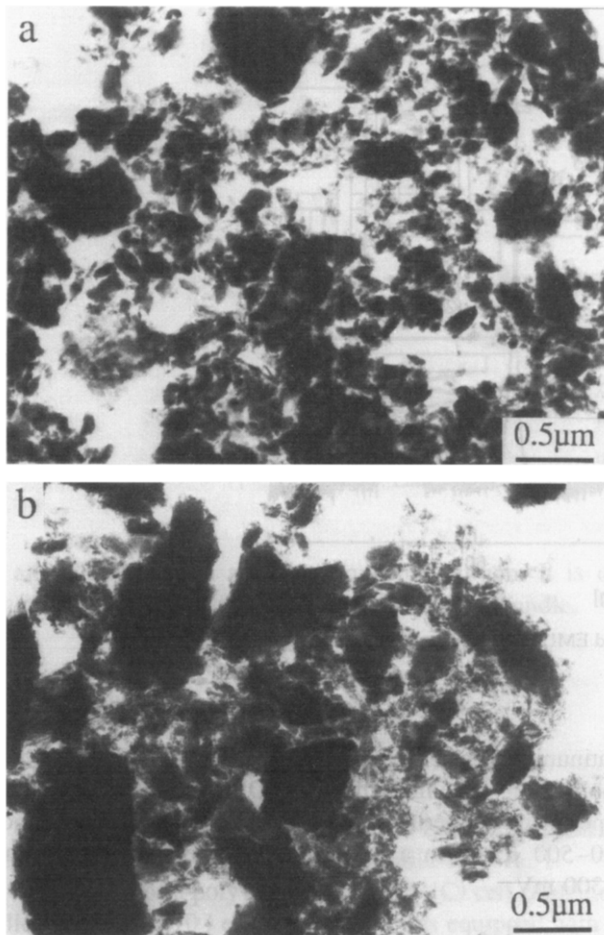


Fig. 5. (a) TEM image of standard EMD (I.C. sample no. 17); (b) TEM image of titanium-doped EMD (laboratory product).

will be assembled with modified EMD. These cells will be cycled and compared with standard (laboratory made undoped EMD) reference cells. The discharge will take place using a 3.9 or 10  $\Omega$  resistor and the cut-off voltage will be 900 mV. The cells are recharged by the voltage limited taper current charging (VLTC) method at 1.72 V. Discharge capacity, discharge time and charge capacity are recorded.

#### 2.4. X-ray and electron-microscopic investigations

X-ray diffraction patterns did not reveal significant differences between doped and undoped EMD samples except a slight shift of some signals (Figs. 3 and 4) [11].

The transmission electron microscope (TEM) was applied for inspection of one sample of titanium-doped EMD (lab-production) and — for comparison — a sample of undoped EMD (industrial production). The TEM investigations were performed with a Philips CM20/STEM operated at an acceleration voltage of 200 kV. The microscope was equipped with a post column imaging filter (GIF by Gatan) which allows both the acquisition of electron energy loss spectra (EELS) and energy-filtered images (EFTEM) [12]. The powder specimens were mounted on holey carbon grids using standard TEM preparation procedures.

The TEM images (Fig. 5) show that the industrial product was generally ground to a smaller grain size and that the grain size distribution was more uniform. The TEM image (Fig. 6(a)) which has been recorded at higher

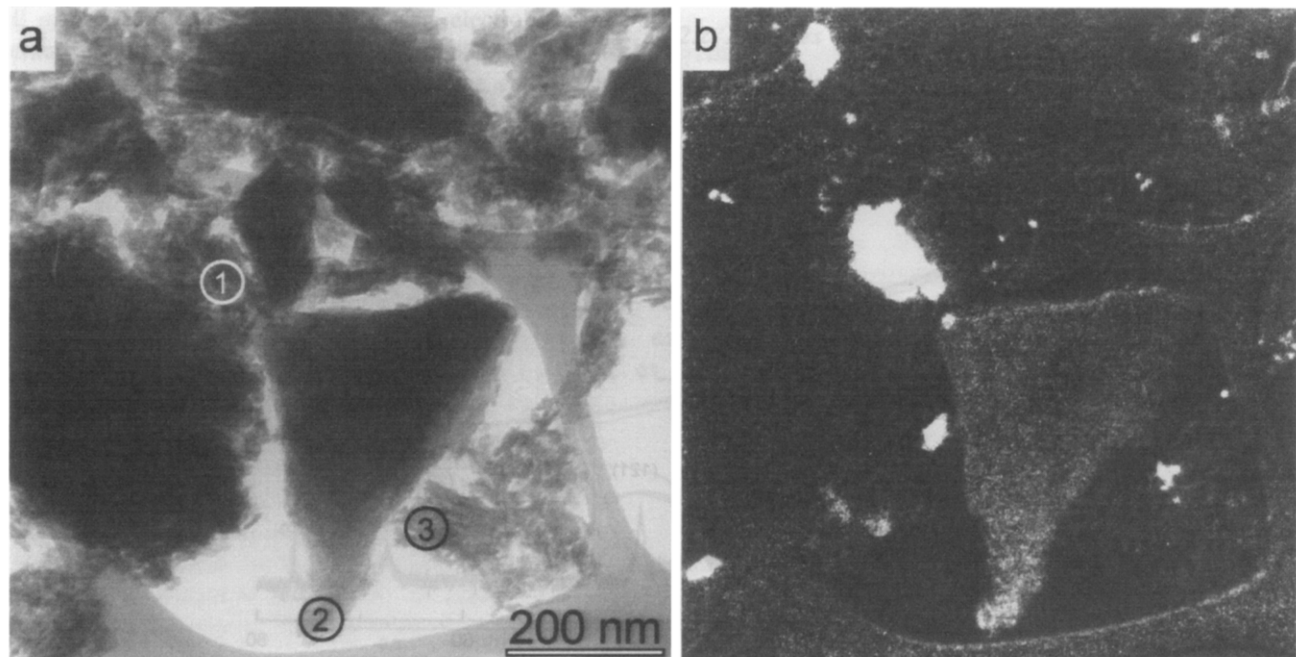


Fig. 6. (a) TEM image of titanium-doped EMD (laboratory product) with higher magnification and areas of EELS spectra indicated; (b) titanium elemental map of the same specimen region as shown in Fig. 6(a).

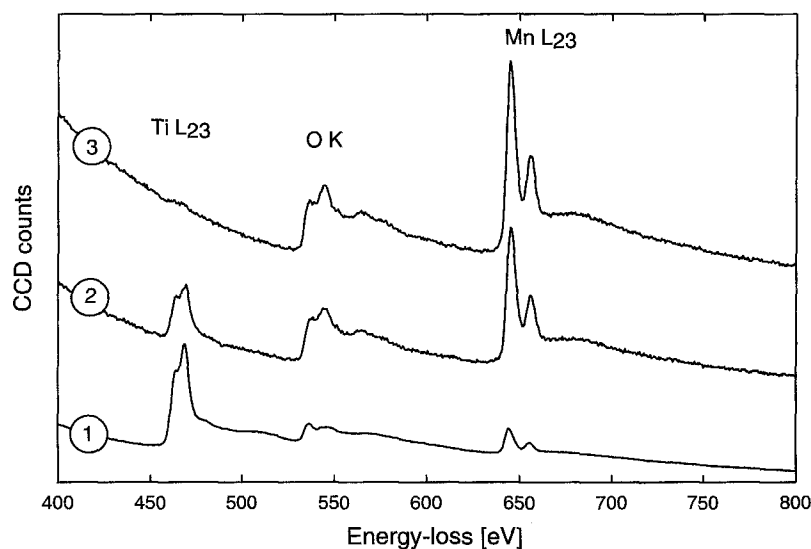


Fig. 7. EELS spectra recorded at the three spots indicated in Fig. 6(a).

magnification reveals a typical specimen region of the titanium-doped specimen. In order to show the distribution of titanium we have recorded energy-filtered images at the Ti  $L_{23}$  ionisation edge. These pre- and post-edge images have been ratioed [13] and the resulting titanium elemental map is shown in Fig. 6(b). This titanium map indicates some agglomerations of titanium-rich material (bright regions) while most of the incorporated titanium is homogeneously distributed. In order to reveal the chemical composition of the various phases, we recorded EELS spectra from the specimen regions marked in Fig. 6(a). These spectra (Fig. 7) exhibit the local chemical composition of the specimen regions and can be also used to derive the local quantitative composition [14]. The spectrum of region 1 corresponds to the titanium-rich bright particle in Fig. 6(b) and the occurrence of the Ti  $L_{23}$ -, the O K- and the Mn  $L_{23}$ -edges show that it is a Ti–Mn-oxide phase. The quantification gives a Ti/O atomic ratio of 0.41 and an Mn/O atomic ratio of 0.27 (Ti/Mn = 2.56). However, in the titanium-map (Fig. 7(b)) small particles with an average diameter of some 10 nm can be also seen. The EELS spectrum of region 2 corresponds to these phases and clearly shows that these particles have a lower titanium concentration. The quantification gives a Ti/O atomic ratio of 0.11 and an Mn/O atomic ratio of 0.60 (Ti/Mn 0.04). The spectrum recorded at the specimen region 3 corresponds to the  $MnO_2$  matrix; it exhibits only a small Ti  $L_{23}$ -edge with a Ti/Mn atomic ratio of about 0.004. Several EELS spectra have been recorded from  $MnO_2$  particles and in all cases we found similar ratios, thus, demonstrating that titanium is homogeneously distributed in the  $MnO_2$  particles. In addition, we found a few small particles (some nm diameter) of spinel composition. Analytical results were equivalent to the formula  $Mn_2TiO_4$ .

Furthermore, it should be mentioned that segregation of pure titanium dioxide could not be found.

### 3. Results and discussion

#### 3.1. Electrodeposition

A summary of the EMD electrodeposition results is given in Table 1.

The process (one batch) was run for approximately 20 h. Each run yielded 150 to 275 g EMD. One reason for the differences in the current efficiency of the process can be associated with the stripping process after the electrolysis. The titanium content of the EMD samples differs between 0.4 and 1.8%. There are several processes that

Table 1  
Results of EMD electrodeposition

Batch number	EMD yield (g)	Current efficiency (%)	Titanium content (%)	Remarks
1	173	65	1.59	product B
2	239	87	0.69	product A
3	242	90	0.88	product A
4	258	92	1.04	product B
5	247	94		a
6	172	66	1.63	product B
7	154	99	0.43	b
8	260	96	0.92	product A
9	265	105	0.95	product A
10	260	100	0.78	product A
11	268	103	0.75	product A
12	275	105	0.83	product A

<sup>a</sup> The product was excluded from further testing due to problems with the electrolyte circulation.

<sup>b</sup> The product was excluded from further testing due to the low titanium content.

may explain the uptake of ions in solution by EMD, occlusion, solid–solution formation and adsorption. Occlusion is unlikely to occur. Solid–solution formation occurs when the lattice structure of the doping metal is similar to that of EMD. The manganese dioxide surface strongly adsorbs metal ions from the solution by ion exchange with protons of surface hydroxyl groups. The adsorbed metal ions form surface complexes which will be converted to oxides when they are enclosed in the bulk of the growing EMD. The codeposition of doping ions can be explained mainly by adsorption processes [15]. The amount of doping ions incorporated into EMD is a function of the metal ion concentration, the kind of metal ion and the current density.

In order to get greater amounts of homogeneously titanium-doped materials, the EMD from batch number 1, 4 and 6 (group B) and from batch number 2, 3, 8, 9, 10, 11 and 12 (group A) were mixed together. The material was shipped to Canada for testing at Battery Technologies.

### 3.2. Electrochemistry

The CV data were collected for different electrolysis products. A typical CV is shown in Fig. 2. The first three cycles of a titanium-doped electrode are displayed.

One major reduction process was resolved during the initial discharge of the electrode. This process has a peak potential of  $-50$  mV. It can be assumed that this broad peak is a result of the homogeneous reduction of  $\text{Mn}^{4+}$  ions in different domains within the EMD structure. The first charge half-cycle showed two main oxidation processes. The first of these processes is a process occurring at a peak potential of  $-220$  mV. It has been suggested [16,17] that this oxidation process corresponds to the oxidation of  $\text{Mn}(\text{OH})_2$  to form a variety of  $\text{Mn}^{3+}$  intermediates including  $\gamma\text{-Mn}_2\text{O}_3$ ,  $\gamma\text{-MnOOH}$  and  $\beta\text{-MnOOH}$ . In the later charge half-cycles the current response of this process increased with cycle number. The second oxidation process observed occurred over a very broad potential range with a peak potential at  $+50$  mV. The fact that this oxidation process covered a wide potential range suggested that it was a homogeneous process. This process is involved in the oxidation of  $\text{Mn}^{3+}$  intermediates to manganese dioxide. The variety of manganese dioxide formed was believed to depend on the  $\text{Mn}^{3+}$  intermediate oxidised. In subsequent reduction half-cycles, the voltammetric data showed peaks at  $-230$  and at  $-430$  mV. A progressive decrease in current response for the reduction process occurring at  $-230$  mV may be observed. This process is believed to be associated with the reduction of  $\text{Mn}^{4+}$  species located in the ramsdellite domains within the EMD structure. An additional peak was observed at  $-430$  mV. This reduction process is believed to involve the reduction of manganese dioxide to  $\text{Mn}(\text{OH})_2$ . The current response associated with this reduction process increased with cycle number. This indicates that the pres-

ence of  $\text{Ti}^{4+}$  affects the electrode by changing the discharge mechanism. It seems that the presence of  $\text{Ti}^{4+}$  ions inhibits the homogeneous reduction and favours the heterogeneous reaction path.

It is difficult to deduce the behaviour of the titanium-doped EMD in battery testing from the results of CV experiments. In CV experiments a half-cell reaction is monitored and it cannot be seen as a simulation of the real battery situation. For example the EMD has no contact with zinc and the complex processes on each side of the separator are not encountered in these experiments.

### 3.3. Battery testing

Testing of the titanium-doped material under real battery conditions will take place in Canada. At BTI the cells will be assembled on a production line and not made manually. This factor usually improves the cell performance but the results have to be compared with those of an undoped EMD equally produced with the same laboratory equipment. Using industry standard EMD as a reference material would give irrelevant results.

## 4. Conclusions

The described laboratory equipment for EMD electrolysis was found useful to produce this material in doped or undoped condition up to 275 g per batch.

Titanium-doped EMD was found to take up an average concentration of the doping element between 0.7 and 1.6%. The major part of this titanium was uniformly distributed but some segregations with significantly higher titanium concentration could be detected. Future experiments will answer the question if a smaller fraction of the doping compound in the electrolyte (less than 16 g/l) during EMD deposition may result in a really homogeneous distribution of titanium in the product.

## Acknowledgements

Grateful acknowledgement is made to the Austrian Research Foundation (Special Research Project ‘Electroactive Materials’) and Battery Technologies Inc., for financial support of this work. The authors are greatly indebted to Röhr and Stolberg GmbH, Krefeld–Linn, Germany, for the supply with lead electrodes and DEKA Rohrsysteme GmbH, Dautphetal, Germany, for all the PVC-C materials.

## References

- [1] K. Kordes, J. Gsellmann, M. Peri, K. Tomantschger and R. Chemelli, *Electrochim. Acta*, 26 (1981) 1495.

- [2] L. Binder, W. Odar and K. Kordesch, *J. Power Sources*, 6 (1981) 271–289.
- [3] K. Kordesch, L. Binder, W. Taucher, C. Faistauer and J. Daniel-Ivad, in A. Attewell and T. Keily (eds.), *Power Sources 14*, International Power Sources Symposium Committee, Leatherhead, UK, 1993, p. 193.
- [4] H.S. Wroblowa, and N. Gupta, *J. Electroanal. Chem.*, 238 (1987) 93.
- [5] B.E. Conway, D.Y. Qu, L. Bai, Y.H. Zhou and W.A. Adams, *J. Appl. Electrochem.*, 23 (1993) 693–706.
- [6] B.E. Conway, L. Bai, D.Y. Qu, Y.H. Zhou, G. Chowdhury and W.A. Adams, *J. Electrochem. Soc.*, 140 (1993) 884–889.
- [7] Y.F. Yao, US Patent No. 4 520 005 (1985).
- [8] R.C. Kainthia and D.J. Manko, US Patent No. 5 156 934 (1992).
- [9] K. Kordesch and J. Gsellmann, DE Patent No. 33 37 568 C2 (1989).
- [10] P. Urdl, Ph.D. Thesis, Technical University, Graz, 1994.
- [11] K. Reichmann, Internal Rep., Technical University, Graz, 1996.
- [12] O.L. Krivanek, A.J. Gubbens, N. Dellby and C.E. Meyer, *Microsc. Microanal. Microstruct.*, 3 (1992) 187–194.
- [13] F. Hofer, P. Warbichler and W. Grogger, *Ultramicroscopy*, 59 (1995) 15–31.
- [14] F. Hofer and P. Golob, *Micron Microsc. Acta*, 19 (1988) 73–86.
- [15] H. Tamura, K. Ishizeki, M. Nagayama and R. Furuichi, *J. Electrochem. Soc.*, 141 (1994) 2035.
- [16] J. McBreen, *J. Power Sources*, 5 (1975) 525.
- [17] S.W. Donne, Ph.D. Thesis, University of Newcastle, Australia, 1996.